

Chapter 6

Effect of Copper Additions on Secondary Carbide Precipitation in High Chromium with Cast Iron

F.V. Guerra, A. Bedolla-Jacuinde, I. Mejía, J. Zuno-Silva,
and E. Cardoso-Legorreta

Abstract This work analyzes the secondary carbide precipitation during the destabilization heat treatment of a 15 % Cr white iron and copper additions between 0.5 and 2 wt%. The destabilization heat treatments were undertaken at temperatures of 850, 950, and 1050 °C between 5 and 480 min. Characterization was carried out by X-ray diffraction (XRD), optical and electron microscopy, image analysis, and energy-dispersive spectroscopy (EDS) microanalysis; the resultant hardness was also measured. It was found that the copper addition resulted in an increase in discontinuity of the eutectic carbide in as-cast conditions. After the heat treatment, the number of precipitated carbides increased with the copper addition, and they were found smaller. There were an increase of precipitation for lower destabilization temperatures and large soaking times.

Keywords High-chromium white cast iron • Destabilization • Precipitation • Secondary carbides • Copper

6.1 Introduction

High-chromium white irons are ferrous alloys containing between 11–30 % Cr and 1.8–3.6 % C carbon, with molybdenum, manganese, copper, and nickel sometimes added as additional alloying elements. The typical as-cast microstructure of these alloys consists of primary and/or eutectic carbides (M_7C_3) in an austenitic matrix or one of its transformation products [1]. The hard eutectic carbides and matrix present

F.V. Guerra (✉) • J. Zuno-Silva • E. Cardoso-Legorreta
Universidad Autónoma del Estado de Hidalgo, Av. Madero 706, Doctores,
42090 Pachuca, Hgo., Mexico
e-mail: vapeani@hotmail.com

A. Bedolla-Jacuinde • I. Mejía
Instituto de Inv. Metalúrgicas y de Materiales, UMSNH. J. Múgica S/N,
58030, Morelia, Mich., México

in the microstructure are responsible for the great abrasion resistance and fracture toughness of these alloys; hence, these alloys are commonly used to applications where abrasion resistance is the main required property [2]. If a high hardness is needed, the as-cast austenitic structure is submitted to destabilization heat treatment between 800 and 1000 °C to obtain small secondary carbides (SC) precipitated in the matrix. During the treatment, the matrix decreases in chromium and carbon content due to precipitation of carbides raising the temperature of martensitic start transformation resulting in a mixture of martensite and retained austenite [3]. Some alloying elements like Cr, Mo, Ni, and Cu are added to promote a good hardenability [4]. Temperature in combination with the soaking time and content of alloying elements change the kinetic of precipitation of secondary carbides. The addition of Cu contributes to hardenability but stabilizes the austenite and delays the carbon diffusion [4]. Therefore, the presence of Cu has a strong influence in the precipitation of secondary carbides modifying the time of precipitation. Time, temperature, and Cu content are the variables used in this work, to analyze their effect on distribution, velocity, and microhardness of precipitated carbides.

6.2 Experimental

The high-chromium white iron subject to experimentation was manufactured with high-purity raw materials to control impurities and chemical composition. They were melted in an induction furnace and poured in a sand mold to obtain bars of 10 in. length and 1 in. diameter. Four different compositions were obtained with 15 % Cr, 3 % C, 1 % Mo, 1 % Ni, and 0, 0.5, 1, and 2 wt% Cu, respectively. The bars were sectioned on samples of $1/2 \times 1/2 \times 1/4$ in. with an abrasive wheel in a Struers metallographic cutter (Struers, Copenhagen, Denmark) Labotom-3 using coolant to avoid overheating. The heat treatments were carried out on an electric furnace at 850, 950, and 1050 °C and soaking times of 5, 15, 30, 60, 90, 150, 300, and 480 min for each composition; the samples were quenched in water to avoid further precipitation during cooling. Samples were prepared for metallography by grinding on abrasive paper of different mesh sizes. Samples were then polished on nylon cloth with 6 μm diamond paste as the abrasive and finally with 1 μm paste. Etching was carried out with two different solutions: Vilella's etchant (5 ml HCl and 1 g picric acid in 100 ml ethanol) for 30–60 s to reveal the microstructure and a solution of 50 ml FeCl₃ plus 20 ml HCl in 930 ml ethanol immersed during 8 h, for a deep etching to remove part of the matrix to observe the eutectic carbides. As-cast eutectic carbide volume fraction was measured by image analysis on digitized micrographs obtained at 200× on a Nikon EPIPHOT 300 optical microscope (Nikon, Melville, NY). For this purpose, the samples were deeply etched, and 20 micrographs were processed by the SigmaScan (Jandel Scientific, San Rafael, CA) V.5 software on a PC. XRD studies were also undertaken to identify the different phases present in the alloy before and after heat treatment. Retained austenite after heat treatment was calculated from XRD data by the technique described by Kim [5]. XRD tests

were carried out by using Cu-K α radiation in a 2θ range of 30–130°. Further characterization was undertaken on a JEOL (JEOL, Peabody, MA) 6400 SEM at 20 kV for imaging and EDS microanalysis. Secondary carbide volume fraction and size were obtained by point counting measurements on SEM micrographs. Microhardness of the matrix was undertaken on metallographic samples. Twenty tests for each sample were carried out by a diamond indenter and a 100 g load for 15 s, for Vickers microhardness (HV100).

6.3 Results and Discussion

The chemical composition of the experimental irons is shown in Table 6.1.

As shown in Table 6.1, the main difference in composition is regarding the copper content. Therefore the changes in microstructure and properties are attributed to copper addition. This copper addition was made to modify the time of precipitation of secondary carbides because it is known that the copper addition can increase the hardenability and decrease the carbon diffusion [6, 7] which modifies the time, shape, and distribution of precipitated carbides.

6.3.1 As-Cast Structure

Figure 6.1 shows the as-cast structure of the alloy, where the eutectic M₇C₃ carbides and the austenitic matrix can be observed; however, small amounts of martensite α' and molybdenum M₂C carbides can be observed.

The presence of martensite can be observed in the periphery of the eutectic carbide due to the carbon and chromium depletion by diffusion to the carbide, which causes the raising of the martensite start temperature (M_s), giving place to the martensitic transformation under cooling to room temperature [3, 8, 9]. The XRD pattern of Fig. 6.2 shows the presence of austenite γ , eutectic carbides M₇C₃, and carbides type M₂C in the alloy; no ferrite/martensite peaks are observed due to the low volume content in as-cast conditions.

The presence of copper precipitate particles or segregation was not observed; as shown in Fig. 6.3, copper is distributed uniformly in the matrix.

The quantification of eutectic carbide volume fraction is shown in Table 6.2.

Table 6.1 Chemical composition of experimental irons, wt%

Alloy	C	Cr	Mo	Ni	Cu
A	2.97	15.21	1.02	1.05	0
B	3.15	14.79	1.01	0.97	0.6
C	3.13	15.47	0.97	0.96	1.1
D	2.96	15.51	0.97	1.04	2.1

Fig. 6.1 As-cast microstructure of the as-cast experimental iron

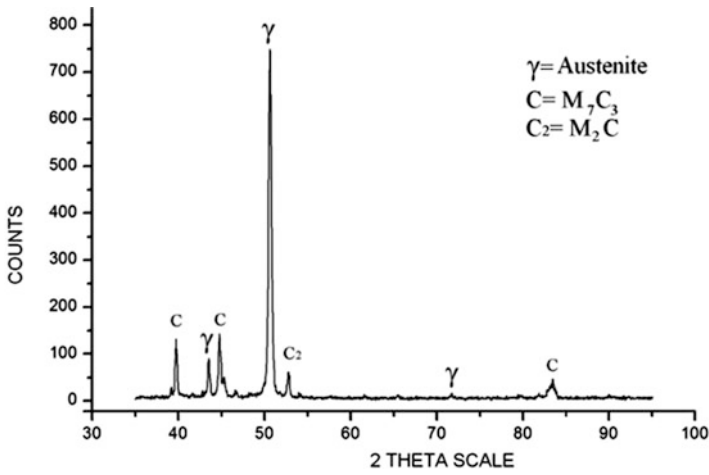
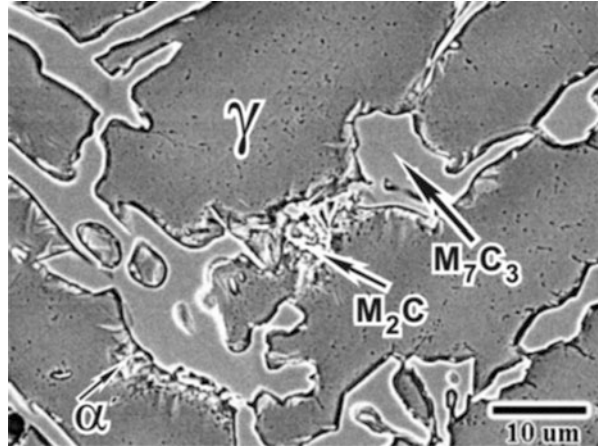


Fig. 6.2 XRD pattern of the D alloy in as-cast conditions

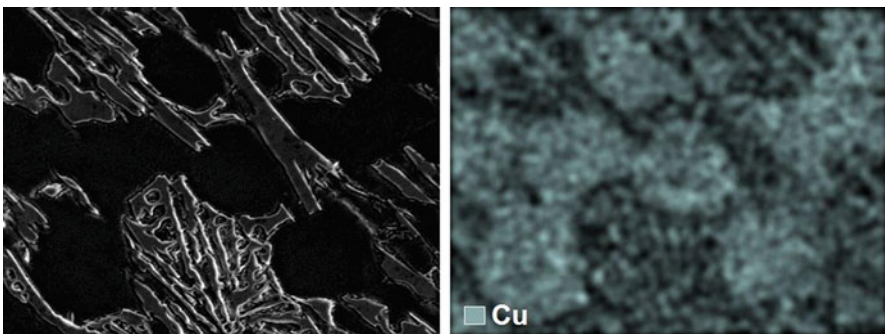
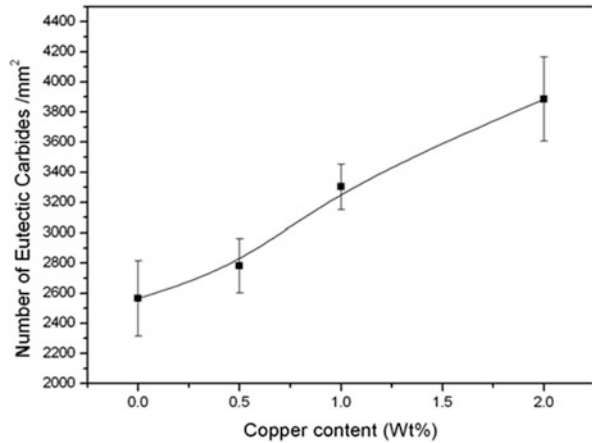


Fig. 6.3 SEM micrograph and chemical composition mapping for copper

Table 6.2 Eutectic carbide volume fraction ($ECV_{Frac.}$)

Cu Wt%	0	0.6	1.1	2.1
$ECV_{Frac.}$	26.5 %	27 %	27.5 %	26.5 %

Fig. 6.4 Eutectic carbides/ mm^2 as a function of copper content

There is no significant difference about the volume fraction of eutectic carbide, but there is a different distribution. Figure 6.4 shows the number of eutectic carbides per square millimeter.

As shown in Fig. 6.4, the number of carbides/ mm^2 increases with increasing the copper addition, but the volume remains almost constant; this is seen as more discontinuous eutectic carbide. The above agrees with the observations of Choi et al. [10] for irons with higher content of copper. This modifying effect has been widely reported for different researchers [11–15] and is based necessarily on segregation during the solidification process, due to the lower solubility on at least one of the phases. Similar effect has been found by Liang and Su [14] in low-chromium white irons, where the addition of 5 wt% of rare earths (RE) changes the leader phase during the solidification process from austenite to cementite. They found cementite blocks instead of a common ledeburitic structure. It seems that the presence of copper limits the growth in certain directions, obtaining a higher number of eutectic carbides with a constant volume. But it not necessarily limits the precipitation; according to Qingxiang et al. [11], rare earth addition suppresses the M_3C growth in a Ni-Cr iron in the [010] direction. Also, they observed that this addition of RE promotes the growing in [100] and [001] directions helping the formation of carbides in the form of isolated blocks.

6.3.2 Structure After Destabilization Heat Treatment

The heat treatment changes the volume of phases, increasing the volume of carbide and martensite at the expense of austenite with the increase in the soaking time, except in those treated at 1050 °C where the austenite phase was overstabilized as will be shown later. The number and size of precipitated carbides are functions of temperature, time, and chemical composition.

6.3.3 Number and Average Diameter of Secondary Carbides

Figure 6.5 shows a sequence of micrographs (a–d) from the iron with 1 % of copper addition, heat treated for 15, 60, 120, and 480 min, respectively, at 850 °C.

From Fig. 6.4, we can observe an increase in precipitation with the increase of the exposure time. Figure 6.5 shows the average number of precipitated carbides per square micrometer. For the different alloys, the average number of precipitated

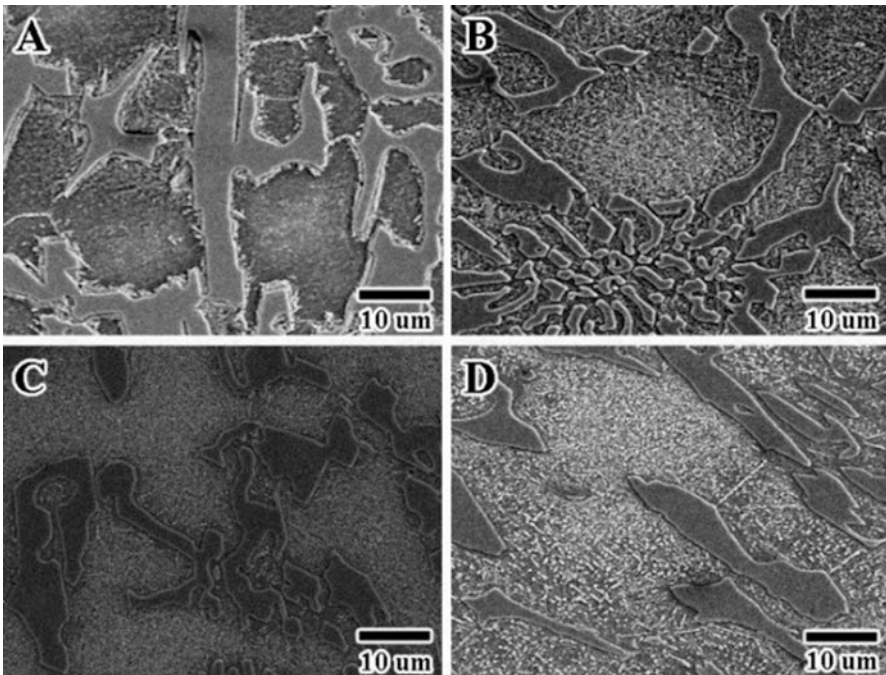


Fig. 6.5 SEM micrographs of 1 % of copper iron heat treated for 15, 60, 120, and 480 min at 850 °C

carbides increases with the holding time at 850 °C; this is because at this temperature, the rate of diffusion to reach the equilibrium is low and the precipitation continued until the longer times.

Therefore, as shown in Fig. 6.4, the microstructures of the heat-treated alloys at 850 °C show a very small-size secondary carbide distribution. Copper additions produce a delay of carbide precipitation for short periods of time as shown in Fig. 6.5 because copper stabilizes the austenite phase in accordance with Krishnadev and Sudan (see JW Choi, 1992) [10]. For holding times longer than 90 min, a remarkable increase in the number of secondary carbides on higher-copper content samples is shown. This effect is attributed to the ability of copper to reduce the diffusion of carbon in austenite; therefore, the elements which form the precipitates (Cr and C) are expelled from the matrix during the destabilization process, and due to the presence of copper, they move shorter distances. As a result, we have a greater number of particles but of smaller size as we can see on Figs. 6.6 and 6.7 with the copper addition.

As we can see, the samples with higher copper content show precipitated carbides with smaller diameter. Figure 6.6 shows that the precipitation occurs in short periods of time in the samples with lower copper content, but there are only some large particles of diameters between 0.20 and 0.25 μm . After the average diameter decreases due to precipitation of particles of smaller size, precipitation continues until 150 min. Subsequently the particles start to grow up to a diameter between 0.17 and 0.19 μm . By contrast, samples with copper contents of 1 and 2 % at longer times of 15 min have precipitated particles of very small diameters of about 0.06 μm . Precipitation occurs in uniformly throughout the matrix. These particles start to grow at times greater than 150 min; this effect is attributed to the copper's ability to decrease the carbon diffusion in austenite. Therefore carbon and chromium expelled from the matrix tend to move shorter distances. As mentioned above the case has been reported by some researchers as Choi et al. [10] in the presence of copper secondary carbides; therefore, it can be acting as nucleating since it has a greater number of smaller precipitates of smaller size.

Fig. 6.6 Number of precipitated carbides as a function of soaking time at 850 °C

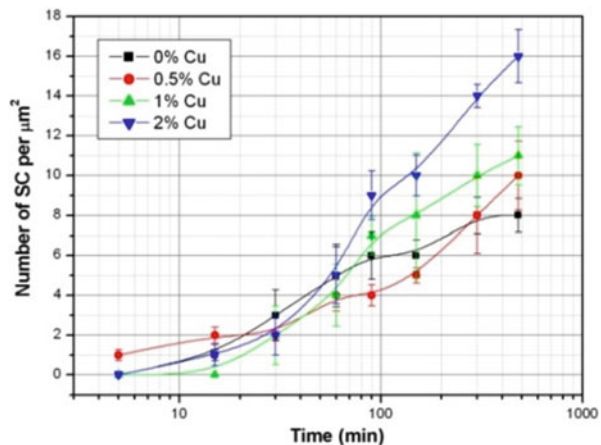


Fig. 6.7 Average diameter of SEC. Carbides as a function of soaking time at 850 °C

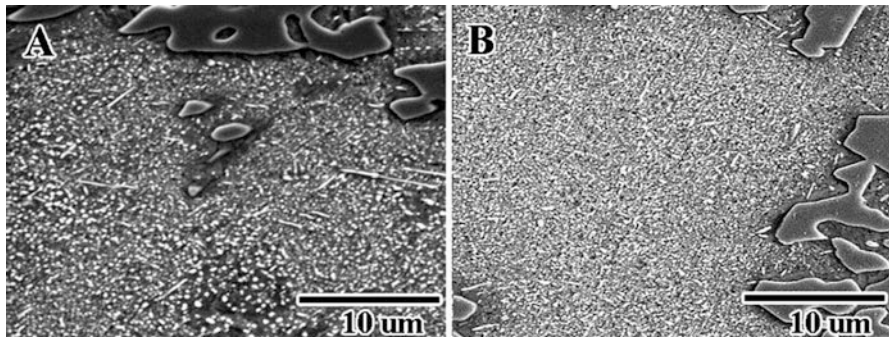
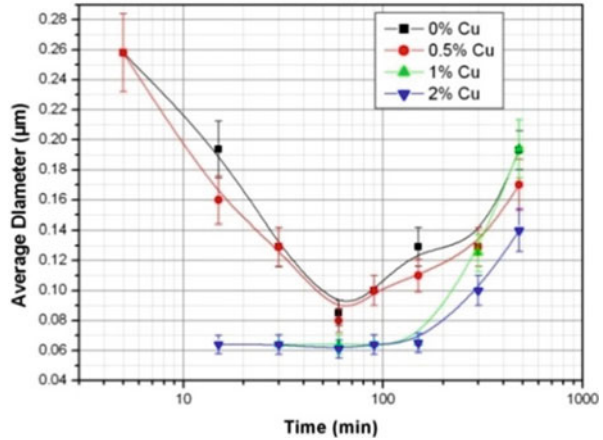


Fig. 6.8 SEM micrographs showing secondary carbide precipitation during destabilization heat treatment at 850 °C. (a) Base alloy, (b) 2 wt% of copper alloyed white iron

Figure 6.8 shows the micrographs for comparative purposes for the alloys treated for 480 min at 850 °C; we can observe a notable increment on the number of precipitated carbides and of smaller size in the 2 % of copper alloy.

Figure 6.9 shows a sequence of micrographs (A–D) from the iron with 1 % of copper addition, heat treated for 15, 60, 120, and 480 min, respectively, at 950 °C.

Figure 6.10 shows the number of secondary carbides precipitated as a function of the soaking time during destabilization at 950 °C.

As we can see, the number of precipitated carbides is lower and reaches a maximum at 90 min and subsequently decreases; this is because the precipitation is performed by nucleation and growth phenomena; at this temperature the diffusion coefficient is higher than at 850 °C. At the temperature of 950 °C, the delayed precipitation is also observed with the increase in the copper content, but as observed in the treatment at 850 °C and after 60 min of treatment, the number of precipitated particles increases notably. As the temperature increases, precipitation occurs in shorter times; this increase in temperature accelerates the diffusion of

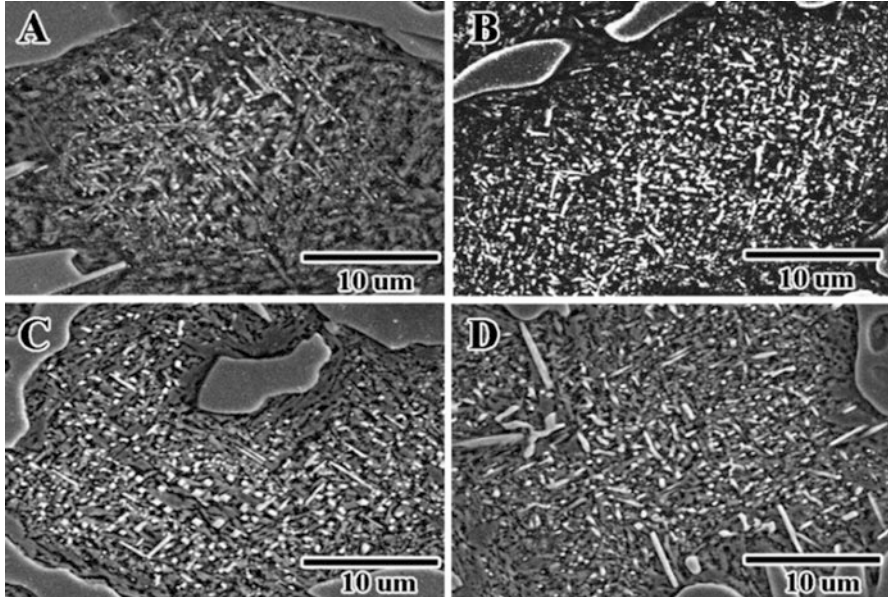
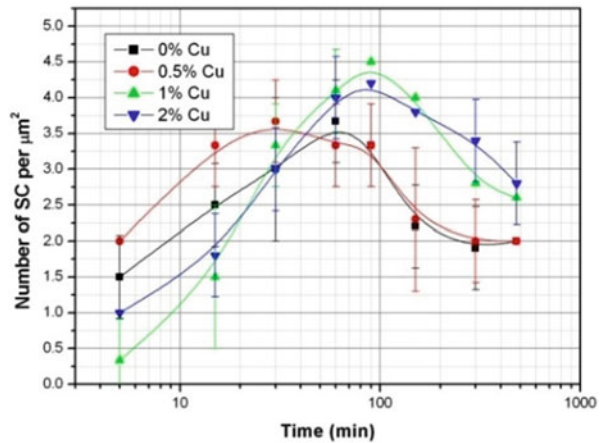


Fig. 6.9 SEM micrographs of the alloy with 1% of copper heat treated for 15, 60, 120, and 480 min at 850 °C

Fig. 6.10 Number of secondary carbides as a function of soaking time at 950 °C



dissolved elements in the matrix. The aforementioned effect is shown in Fig. 6.11 where precipitated carbides are observed for two samples of the same composition. Figure 6.11a corresponds to the sample heat treated at 850 °C and Fig. 6.11b at 950 °C; we can observe the reduction in number of precipitates but an increase in size due to increased diffusivity. The average diameter of the precipitated carbides at 950 °C is shown in Fig. 6.12.

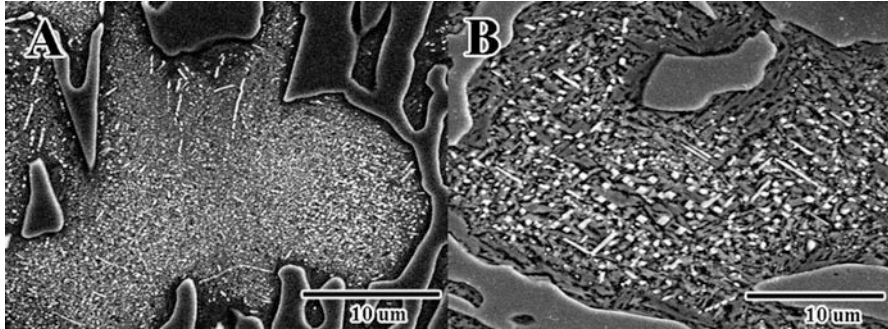


Fig. 6.11 Comparative micrographs of 1% copper alloyed iron heat treated for 300 min. (a) 850 °C, (b) 950 °C

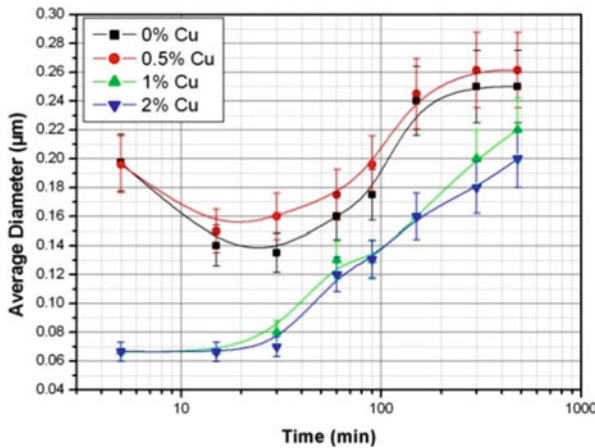


Fig. 6.12 Average diameter of precipitated carbides as a function of soaking time at 950 °C

As observed at 850 °C, in the samples with lower copper addition, the precipitation occurs in short periods of time, but there are only some large particles of diameters; after, the average diameter decreases due to the precipitation of particles of smaller size; after 30 min, the present particles start growing. In the case of the samples with copper contents of 1 and 2 %, the precipitated particles are of small diameter, precipitation continues until 90 min, and then the particles begin to grow; the average diameter is small and the particles are uniformly distributed. Compared with treatment at 850 °C, the average diameter is significantly higher; this is because, as temperature increases, the elements that precipitate from the matrix can travel longer distances and can form bigger carbides due to increased diffusion; therefore, carbides reach an average diameter of up to 0.262 μm in the longer treatment times. The average diameter is greatly increased in comparison with the treatment at 850 °C, wherein the average maximum diameter reached at

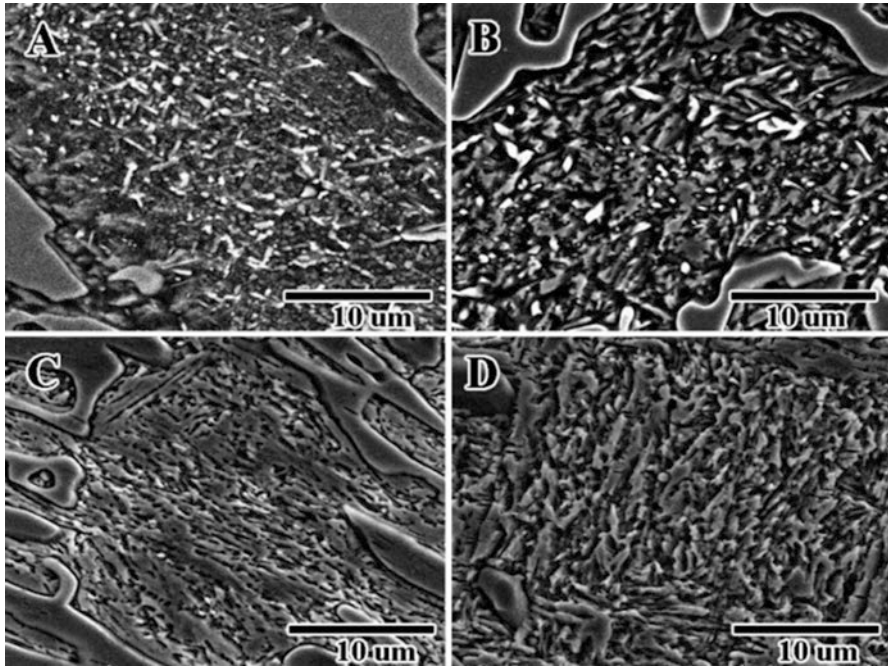


Fig. 6.13 SEM micrographs of the alloy with 1% of copper heat treated for 15, 60, 120, and 480 min at 1050 °C

480 min was 0.19 μm . Figure 6.13 shows a sequence of micrographs (a–d) from the iron with 1% of copper addition, heat treated for 15, 60, 120, and 480 min, respectively, at 1050 °C. We can observe the presence of secondary carbides for short times, but after 60 min, there is a decrease in the number; for exposure times longer than 90 min, the matrix is almost free of secondary carbides.

Figure 6.14 shows the quantification of a number of secondary carbides per μm^2 ; precipitation is observed for short times. Complementarily, Fig. 6.15 shows the average diameter of the precipitated carbides at 1050 °C; the average diameter of the precipitates found in short periods of time was significantly greater than those observed at 850 and 950 °C. However, at times over 300 min, the matrix is substantially free of precipitates, as shown in micrographs c and d of Fig. 6.13.

It is possible that the secondary carbides observed at times below 300 min are precipitated during heating, aided by the segregation product of the solidification process, but these dissolve at longer times when the equilibrium composition of carbon and chromium in the austenite is reached. It is possible that at this temperature, the equilibrium concentration of carbon in austenite can be higher than the carbon content that is dissolved in the matrix. In support of the above assertion, Fig. 6.16 is presented where the dissolution of eutectic carbides is observed, which has not been reported by other researchers; according to Tabrett [1], eutectic carbides are not affected at the destabilization temperatures.

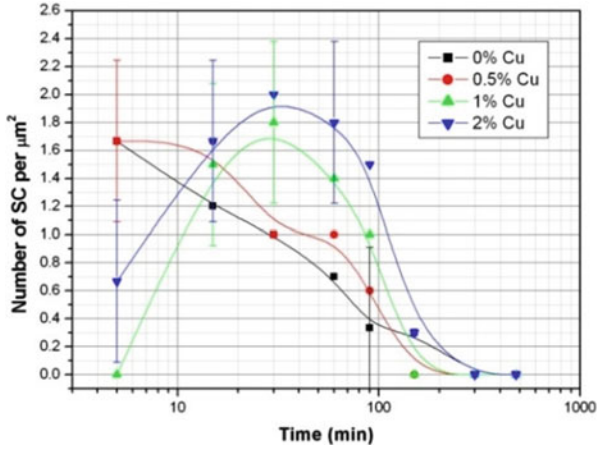


Fig. 6.14 Number of SEC carbides as a function of the soaking time at 1050 °C

Fig. 6.15 Average diameter of SEC carbides as a function of soaking time at 1050 °C

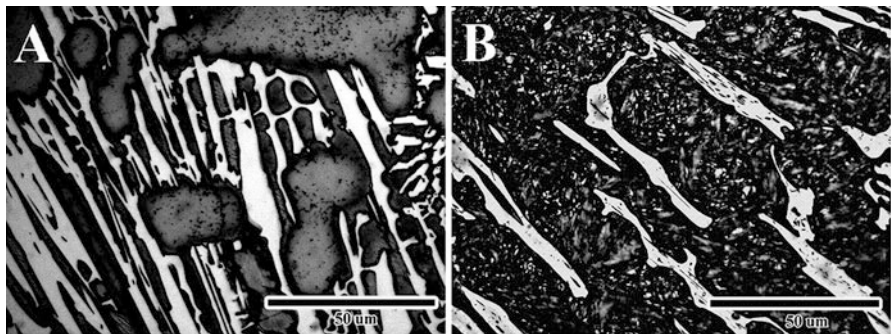
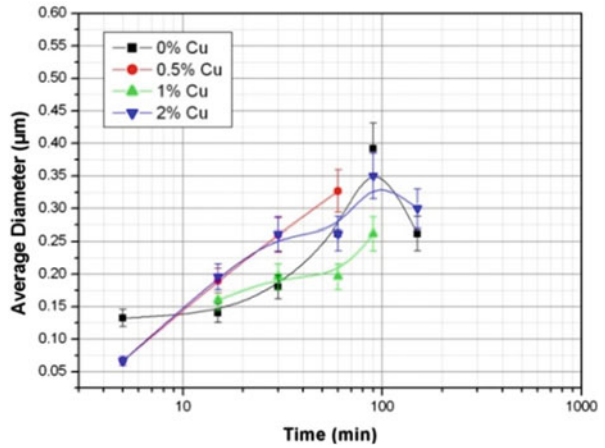
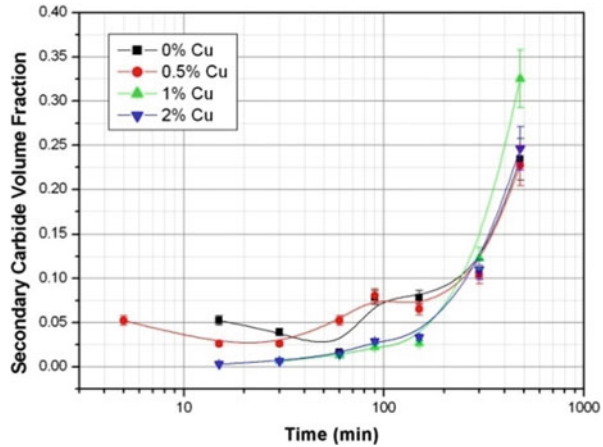


Fig. 6.16 SEM micrographs of the alloy with 2 % of copper: (a) as-cast conditions (b) heat treated at 1050 °C for 480 min. Note the decrease in volume of the iron carbides

Fig. 6.17 SCV_{Frac} as a function of the soaking time at 850 °C



The reason why increasing the treatment temperature decreases precipitation of secondary carbides is explained by the Fe-C diagram. The austenite can dissolve a larger amount of carbon as the temperature increases until the eutectic; this decreases the amount of carbon that can be ejected to form secondary carbides.

6.3.4 Secondary Carbide Volume Fraction (SCV_{Frac})

From measurements of the number and diameter of precipitate carbides, precipitates, calculation of the SCV_{Frac} was performed. The results are presented below. The SCV_{Frac} for the samples thermally treated at 850 °C is shown plotted against time in Fig. 6.17.

It is noted that the volume fraction of carbide precipitates increases with exposure time in the thermal treatment for four different compositions. It is also noted that at short times, the volume of secondary carbides is lower in samples with higher copper content. For times greater than 150 min, the samples with higher copper content increase their SCV_{Frac} .

The maximum volume of 32.5 % was obtained by the sample with 1 % copper, which agrees with the results obtained by Bedolla et al. [16] in a white iron with 2.6 % C, 17 % Cr, 2 % Mo, and 2 % V. It is possible that the measurement results of SCV_{Frac} for the samples with lower copper content have been influenced by the carbon and chromium migration to coarsening the eutectic carbide; therefore, the SCV_{Frac} was lower for this samples.

As can be seen in the micrograph of Fig. 6.7a, there is a darker secondary carbide free region in the vicinity with the eutectic carbide; such region is depleted of chromium and carbon, which has also been observed by Duppin et al. [17] in some high-chromium irons. By contrast, in the samples with higher copper content, this phenomenon is not as evident, which is attributed to the ability of copper to

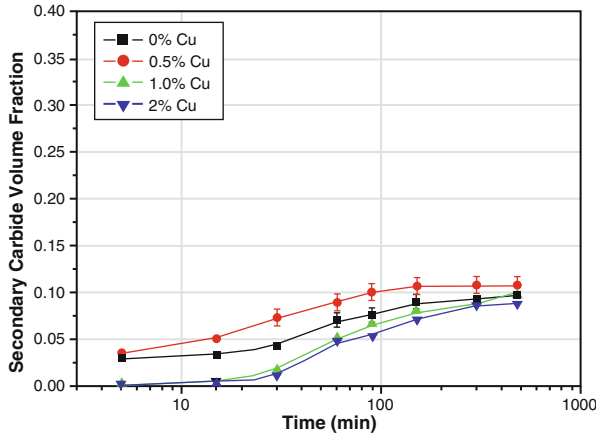


Fig. 6.18 $SCV_{Frac.}$ as a function of the soaking time at $950\text{ }^{\circ}\text{C}$

reduce the diffusion of carbon in austenite forming a diffusion barrier preventing the migration of carbon to the eutectic carbide during solidification. A similar phenomenon has been observed in nodular iron with the addition of copper, where this element segregates at austenite-graphite interface acting as a barrier to the diffusion of carbon into graphite nodules [18]. Figure 6.18 shows the $SCV_{Frac.}$ for the samples heat treated at $950\text{ }^{\circ}\text{C}$.

As was observed in the treatment at $850\text{ }^{\circ}\text{C}$, there is an increase in the $SCV_{Frac.}$ as the time increases. It is appreciated that the $SCV_{Frac.}$ increases faster than treatment at $850\text{ }^{\circ}\text{C}$; this is because the increase in temperature causes an increase in the diffusion. However, the $SCV_{Frac.}$ is much lower; this is caused by an increased solubility of carbon in austenite which decreases precipitation. Figure 6.19 corresponds to the measurement of $SCV_{Frac.}$ for the treatment at $1050\text{ }^{\circ}\text{C}$.

The $SCV_{Frac.}$ is diminished by the increased solubility of carbon in austenite; therefore, it is remarkably lower compared with the previous two temperatures. In addition for longer times up to 90 min, it is observed that $SCV_{Frac.}$ is almost null. Noticeably as the temperature increases, there is a lower precipitation, since according to the Fe-C diagram, the austenite phase can dissolve higher amount of carbon at higher temperatures until the eutectic. This is reflected in the decrease in volume of secondary carbides precipitated. In contrast at lower temperatures, the capacity of austenite for dissolving carbon is lower, so there is greater amount of carbon to precipitate, which is reflected in a higher volume of secondary carbides.

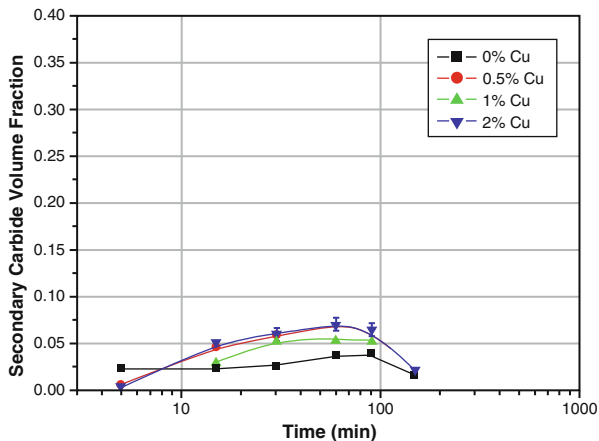


Fig. 6.19 SCV_{Frac.} as a function of the soaking time at 1050 °C

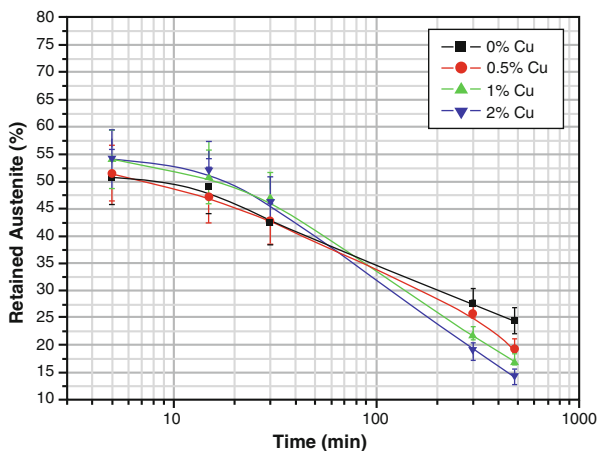


Fig. 6.20 Retained austenite volume fraction as a function of soaking time at 850 °C

6.3.5 Retained Austenite Volume Fraction

The results of the measurement of retained austenite after heat treatment are shown in Figs. 6.20, 6.21, and 6.22 heat treated at 850, 950, and 1050 °C, respectively.

In a general way, the samples treated at 850 °C for 480 min show low retained austenite values. The increase in exposure time at this temperature results in a higher precipitation of secondary carbides, thereby decreasing the volume of retained austenite, since as the treatment time increases, the matrix is reduced in dissolved alloying elements, which increases the volume of material to be transformed to martensite during subsequent cooling. As mentioned above, the precipitation of

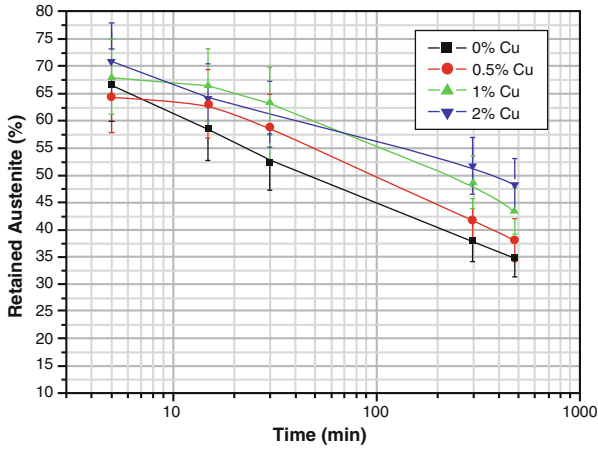


Fig. 6.21 Retained austenite volume fraction as a function of soaking time at 950 °C

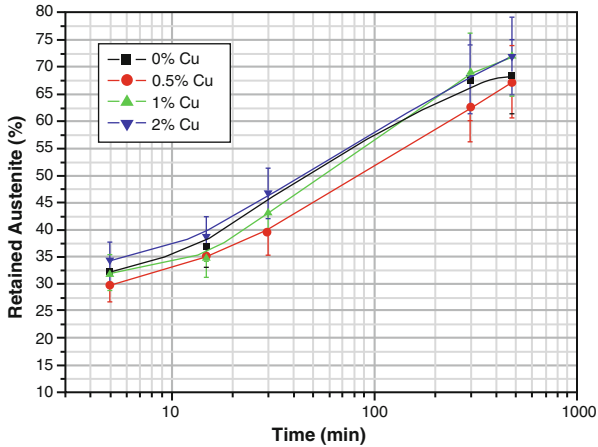


Fig. 6.22 Retained austenite volume fraction as a function of soaking time at 1050 °C

secondary carbides during heat treatment depletes the austenitic matrix in carbon and chromium mainly [5, 19]. Such depletion in dissolved alloying elements in the matrix causes an increase in the M_s temperature, so martensitic structures are present.

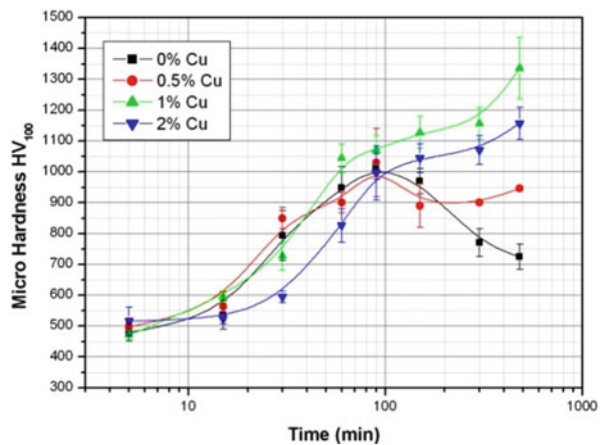
The same trend can be seen in Fig. 6.21, which corresponds to the thermal treatment at 950 °C. However, at this temperature, there is a greater volume of retained austenite compared to treatment at 850 °C. This is explained using the iron-carbon diagram, where at higher temperature austenite can dissolve more carbon, causing a lower precipitation of secondary carbides. Therefore, by increasing temperature, a greater amount of chromium and carbon is dissolved in the matrix,

which lowers the M_s temperature, obtaining thus a larger volume of retained austenite at room temperature. It has been widely reported by several researchers [8, 16, 20, 21]. The retained austenite volume fraction decreases with increasing the exposure time for the four compositions; therefore, the minimum volume of retained austenite occurs in the maximum time of 480 min. In Fig. 6.9 that was showed above, it was observed that the number of secondary carbides decreases, but the precipitation of elements of the matrix continues to give rise to the growth of existing particles; therefore, the residual austenite decreases due to depletion of chromium and carbon matrix which raises the M_s transformation temperature, transforming the matrix to martensite during cooling. In the graph of Fig. 6.22, it shows the retained austenite volume fraction in the iron treated at 1050 °C; it is noted that the austenite volume increases with increasing the soaking time in the heat treatment. This is explained as follows: As the treatment temperature increases, there is a greater dissolution of chromium and carbon in austenite, which stabilize the matrix. Therefore, the austenitic structure is stable during cooling due to the high content of dissolved alloying according to Kim [5].

6.3.6 Microhardness of Matrix After Destabilization

Figure 6.23 shows the microhardness values obtained for the iron matrix after heat treatment. At a temperature of 850 °C, for a treatment time of 5 min, the four compositions practically start with a hardness value around 500 HV₁₀₀; microhardness for all compositions increases with increasing time. Samples with the lower copper content reach a maximum hardness at 90 min, achieving hardness between 1017 and 1030 HV₁₀₀. For times greater than 150 min the hardness decreases as the secondary carbides grow and begin to diminish in number. Furthermore, the samples

Fig. 6.23 Vickers microhardness of the iron matrix as a function of soaking time at 850 °C



with higher copper content continue to harden; this is because in these samples precipitation process starts more slowly. The carbides are of very small size and uniformly distributed; therefore, these reach values of hardness until 1336 HV₁₀₀.

According to the above exposed, the increase in the microhardness values as the treatment time increases is explained by the precipitation of secondary carbides which harden the matrix and the increase in the martensite content. The decrease of the hardness after 150 min in the samples with lower copper content is attributed to the coarsening of carbides, since long exposure times produce an increase in diffusion of elements, resulting in growth of carbides from the dissolution of others. Furthermore, this decrease in hardness is attributed to the formation of martensite of low carbon content due to the low solubility of carbon in austenite and the high precipitation of secondary carbides. The secondary carbides present in the samples treated at 950 °C are much larger than those observed at 850 °C, and although the precipitation decreases, the hardness is only slightly lower than that obtained at 850 °C; further to 850 °C the hardness of the matrix decreases drastically after 90 min for samples with lower content of copper due to the formation of martensite of low carbon content; this phenomenon has been reported by Maratray [22] and Karantzalis [23] (0.31 Ni, 0.47 Cu); both obtain lower hardness values at low temperatures. At 950 °C this phenomenon does not occur due to a lower precipitation; the hardness is maintained between 900 and 950 HV₁₀₀. In the case of samples with higher copper content, the precipitation is slower, but the precipitated particles are smaller. This precipitation continues until long times, resulting in a saturated matrix of fine secondary carbides uniformly distributed increasing the hardness of the matrix.

The described effect is attributed to the addition of copper, which, as mentioned above, reduces the diffusion of carbon in austenite, causing it to move shorter distances. Some researchers as Choi et al. [10] have reported the presence of copper in the secondary carbides, so it is believed that copper may act as nucleating causing a remarkable increase in the number of precipitates. Figure 6.24 shows the microhardness of the matrix for the treatment of 950 °C where there is a peak for samples with lower contents of copper in 60 min and 90 min for the samples with higher copper content, which coincide with the maximum values in the number of secondary carbide precipitates. Then the hardness of the matrix has a slight decrease, due to the growth of these particles. The highest values of microhardness are obtained due to the increase in the volume of martensite.

The maximum hardness value was obtained for samples with lower copper content, reaching a maximum of 975 HV₁₀₀ for a time of 60 min in the sample with 0.5 % Cu.

The above effect at 850 °C due to copper addition is no longer observed, even when it has a greater number of precipitates in samples with higher copper content; the temperature increase produces a greater diffusion, so that the precipitated particles tend to grow rapidly, decreasing the hardness matrix. The decrease in hardness of the matrix compared to treatment at 850 °C is because the amount of precipitated carbides at 950 °C is lower, since the austenite phase can retain in solution higher quantities of carbon and chromium.

Fig. 6.24 Vickers microhardness of the iron matrix as a function of soaking time at 950 °C

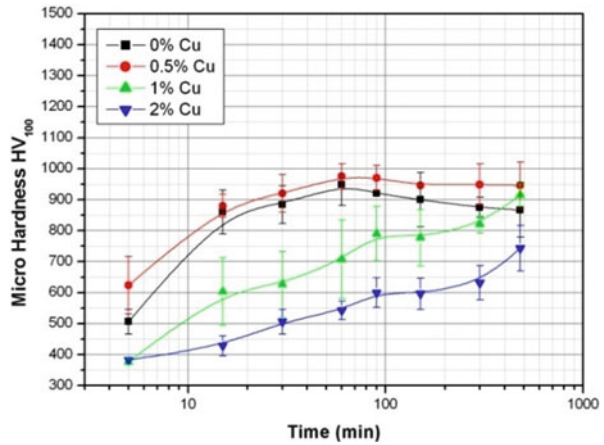
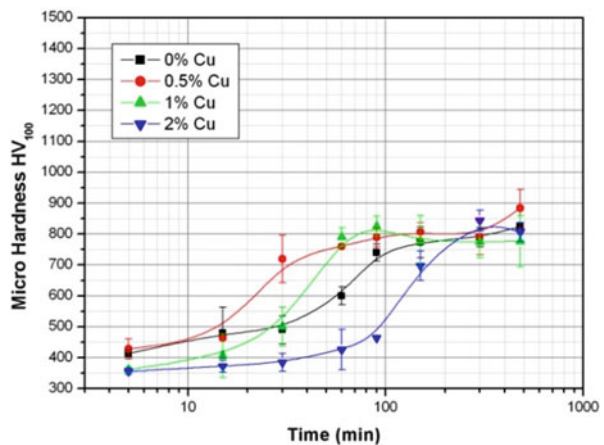


Fig. 6.25 Vickers microhardness of the iron matrix as a function of soaking time at 1050 °C



By increasing the treatment temperature, the formation of a fewer number of nuclei of larger size due to the increased diffusion was observed, allowing the atoms to travel longer distances. This causes a lower precipitation hardening, due to the morphology and distribution of these particles. The lower precipitation of secondary carbides regarding at 1050 °C implied a higher content of retained austenite in the structure reaching lower hardness values in the matrix. Figure 6.25 shows the microhardness values on the heat-treated iron matrix at 1150 °C. In this case we found a phenomenon that has not been reported before during destabilization: the matrix microhardness increased with the soaking time without secondary carbide precipitation.

Unlike the other two temperatures, the volume of residual austenite was increased with time; therefore, for long exposure times, there is not precipitation of secondary carbides and therefore decrease in hardness would be expected. However, hardening was due to solid solution of carbon and chromium, due to the dissolution of part of

the eutectic carbide. At 1050 °C the maximum hardness of the matrix was of 884 HV₁₀₀ for the sample with 0.5 % copper treated by 480 min. For short periods of time, samples with higher copper content show lower microhardness values, and on the previous temperatures, a delay in the precipitation of secondary carbides is observed. However, for long times, the difference is not significant, because all the samples show an almost fully austenitic matrix absent of secondary carbides, hardened only by solid solubility of elements such as carbon and chromium mainly. The above-explained phenomenon was showed previously in Fig. 6.15. In this case, a stabilization of the austenite phase at longer times has led to a structure free of secondary carbides, which was only hardened by solid solution with elements such as carbon, chromium, and molybdenum from the eutectic carbide dissolution.

6.4 Conclusions

Copper additions resulted in more discontinuous eutectic carbide in as-cast condition. After the heat treatment, an increase in number of precipitated particles for lower temperatures of treatment was observed. The smaller diameter of secondary carbides and a more uniform distribution of these were observed in samples with the greater contents of copper heat treated at 850 °C. The volume fraction of secondary carbides was found to increase for lower destabilization temperatures and large holding times. The volume fraction of retained austenite increased as the temperature of treatment was increased; therefore, very low carbide precipitation along with a stabilization of the austenite phase occurred for heat treatment at 1050 °C; in addition, for large soaking times, dissolution of eutectic carbides was observed. Microhardness was observed to decrease with the temperature of heat treatment due to the decrease of secondary carbides and therefore a lower transformation level of austenite to martensite.

Acknowledgements The authors acknowledge the CIC-UMSNH (grant No. 019) and CONACYT (grant No. 57197-Y) for the financial support and UAEH for the facilities obtained during the present research.

References

1. Tabrett CP, Sare IR, Gomashchi MR (1996) Microstructure-property relationships in high-chromium white iron alloys. *Int. Mater Rev* 41(2):59–82
2. Dogan ON, Hawk JA, Laird F II (1997) Solidification structure and abrasion resistance of high chromium white irons. *Metall Mater Trans A* 28(6):1315–27
3. Laird G II, Powell GLF (1993) Solidification and solid-state transformation mechanisms in Si alloyed high-chromium white cast irons. *Metall Trans A* 24(2):981–988
4. Laird G, Gundlach R, Rohrig K (2000) Abrasion resistant cast iron handbook. American Foundry Society, Des. Plaines

5. Kim C (1979) X-Ray method of measuring retained austenite in heat treated white cast irons. *J Heat Treat* 1(2):43–51
6. Babu SS, Bhadeshia HKDH (1995) Diffusion of carbon in substitutionally alloyed austenite. *J Mater Sci Lett* 14:314–316
7. Silman GI, Kamynin VV, Goncharov VV (2007) On the mechanisms of copper effect on structure formation in cast iron. *Met Sci Heat Treat* 49:387–393
8. Powell GLF, Laird G II (1992) Structure, nucleation, growth and morphology of secondary carbides in high chromium and Cr-Ni white cast irons. *J Mater Sci* 27:29–35
9. Laird G II (1991) Microstructures of Ni-Hard I, Ni-Hard IV and High-Cr White Cast Irons. *AFS Trans* 99:339–357
10. Choi JW, Chang SK (1992) Effects of molybdenum and copper additions on microstructure of high chromium cast iron rolls. *ISIJ Int* 32(11):1170–1176
11. Qingxiang Y, Bo L, Jianhua L, Mei Y (1998) Effect of rare earth elements on carbide morphology and phase transformation dynamics of high Ni-Cr alloy cast iron. *J Rare Earths* 16:36–40
12. Shen J, Zhou QD (1988) Solidification behavior of boron-bearing high-chromium cast iron and the modification mechanism of silicon. *Cast Met* 2:79–85
13. Li J, Smith RW (1997) Growth modification of austenite-(Fe,Cr)₃C pseudo-binary eutectic. In: *Proceedings IV Decennial International Conference on Solidification Processing*, pp 481–488
14. Liang GY, Su JY (1992) The effect of rare earth elements on the growth of eutectic carbides in white cast irons containing chromium. *Cast Met* 4(2):83–88
15. Fusheng H, Chaochang W (1989) Modifying high Cr-Mn cast iron with boron and rare earth-Si alloy. *Mater Sci Technol* 5:918–924
16. Bedolla-Jacuinde A, Arias L, Hernández B (2003) Kinetics of secondary carbides precipitation in a high-chromium white iron. *J Mater Eng Perform* 12(4):371–382
17. Duppini P, Saverna J, Schissler JM (1982) A structural study of chromium white cast iron. *AFS Trans* 90:711–718
18. Yu SK, Loper Cr Jr (1988) The effect of molybdenum, copper, and nickel on the pearlitic and martensitic hardenability of ductile cast irons. *AFS Trans* 96:811–822
19. Cias WW (1974) Austenite transformation kinetics and hardenability of heat treated 17.5%Cr white cast irons. *AFS Trans* 82:317–28
20. Kuwano M, Ogi K, Sawamoto A, Matsuda K (1990) Studies on precipitation process of secondary carbides in high-chromium cast iron. *AFS Trans* 98:725–734
21. Powell GLF, Bee JV (1996) Secondary carbide precipitation in an 18 wt%Cr-1 wt%Mo white iron. *J Mater Sci* 31:707–711
22. Maratray F, Poulalion A (1982) Austenite retention in high chromium white irons. *AFS Trans* 90:795–804
23. Karantzalis AE, Lekatou A, Diavati E (2008) Effect of destabilization heat treatments on the microstructure of high-chromium cast iron: a microscopy examination approach. *J Mater Eng Perform* 18(8):1078–1085